

A FINITE ELEMENT STUDY OF OSTHEOSYNTHESIS PLATES

Lucas Lisboa Vignoli, Mechanical Eng. Dept., Catholic University of Rio de Janeiro, PUC-Rio, R. Marques de São Vicente 225, Gávea, Rio de Janeiro, RJ, Brazil, 22451-900, lucas.lvig@gmail.com

Paulo Pedro Kenedi, PPEMM- Programa de Pós-Graduação em Engenharia Mecânica e Tecnologia de Materiais - CEFET/RJ - Av. Maracanã, 229 - Maracanã - RJ - CEP 20271-110, pkenedi@cefet-rj.br

Abstract. *The main function of an osteosynthesis plate is to provide stability to the bone during the healing process. As the plate works in parallel arrangement with bone, the plate has to resist to a parcel of the load, which is proportional to its stiffness. This helps the bone consolidation during the healing process. In this paper a finite element model of a plate fixed at bone medial region with six screws is proposed. The model uses a real femur geometry and a reasonable model for muscle forces. The results are presented using von Mises equivalent stress criterion through various plate paths.*

Keywords: *osteosynthesis plate, finite element, femur.*

1. INTRODUCTION

Osteosynthesis plates, called now on as plates, are important apparatus to assist patients who had broken a bone, as a femur. The forces considered in this study are presented at Fig. 1.a. This loading model configuration, with four external static forces applied at femur's head, was adapted from the Taylor's fourth load case of human left femur's head (Taylor, 1996). Some analytical models, considering a simplified geometry, have been proposed to describe the action of these forces and their moment on the medial section of the system (plate + bone) as in (Kenedi and Riagusoff, 2015). In this work the finite element method, from now on called F.E. method, is used. The F.E. models can represent in a more realistic way than analytical models, the complex geometries of real human long bones.

Figure 1.a shows the F.E. model of a human femur bone with proximal loading and plate installed at medial region. The external forces were named: Joint Reaction (P_A), Abductors (P_B), Ilioopsoas (P_C) and Ilio-Tibial Tract (P_D). See (Bitsakos et al., 2005) for more complex muscle loading cases description. At Fig.1.b it is possible to realize the plate inclination and that the non-constant distance between plate and bone caused by femur bone irregular external shape. At Fig. 1.b shows the utilizizations of six screws to attach the plate on the bone.

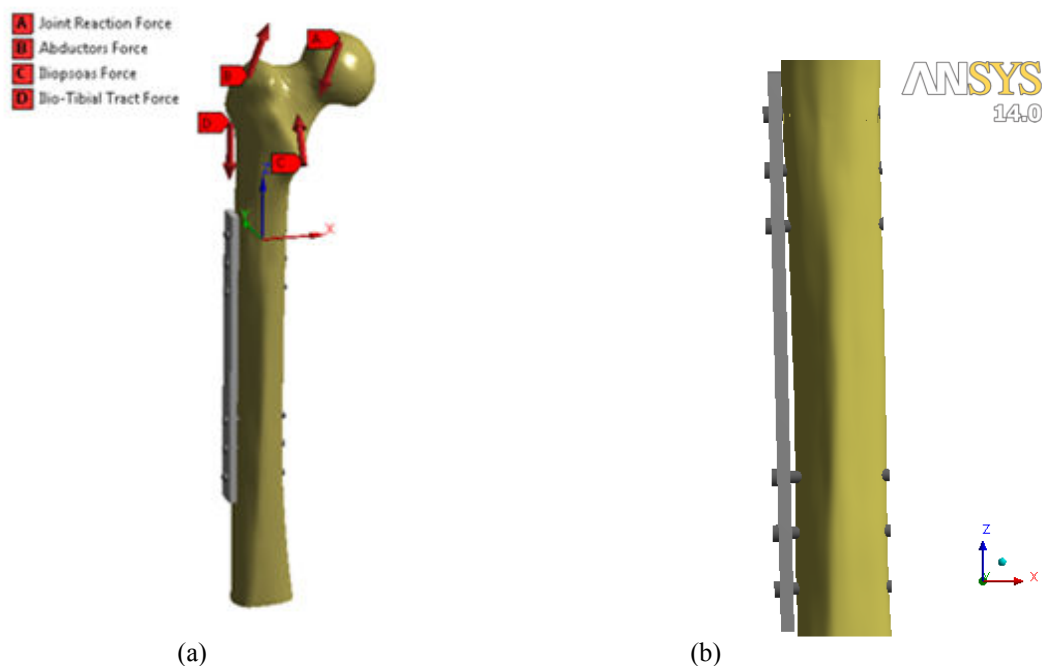


Figure 1. A human femur with a medial plate: (a) general view and (b) detailed view.

At Fig.1.b it is possible to realize the plate inclination and that the non-constant distance between plate and bone caused by femur bone irregular external shape. At next section the F.E. model will be explained.

2. FINITE ELEMENT MODEL

The numerical model was built up using the F.E. software ANSYS, to simulate the effect of the muscles loads acting on the bone/plate set. The simulations were carried out using a few hypotheses, as: The contact between plate and bone is frictionless; the contact between the screw and the bone not allow separation neither slip on their surfaces; the screw and plate contact region also is defined as without normal relative displacement between the faces but frictionless for tangential displacement (the internal surface of the plate hole and the external screw surface are smooth) and the bolt preload is enough to fix the plate.

Figure 2 shows the mesh used at many parts/regions of the numerical simulation. The bone head mesh was less refined than the medial bone region, based on previous paper (Kenedi et al., 2014), where the green line shown at Fig. 2.a separates the head, with element size of 2.5 mm, and the body, with element size of 2.0 mm. For both femur parts, element with midside nodes was adopted, SOLID186 and SOLID187. For the plate mesh it was chosen to use simpler elements as SOLID285 and SOLID18, decreasing the element size to 1mm. The sphere of influence tool was used to refine the plate mesh near the hole, with radius equal to 5 mm and the element size 0.25mm inside this sphere, as shown at Fig. 2.b.

The screw mesh used the elements SOLID285 and SOLID185 with 1.5mm size, except at the external surface where the bolt pretension are applied, which was used the element PRETS179 with 0.25mm size. All the mesh dimensions were adopted after a convergence study. A total of 200827 solid elements, 79639 contact elements and 330695 nodes were used.

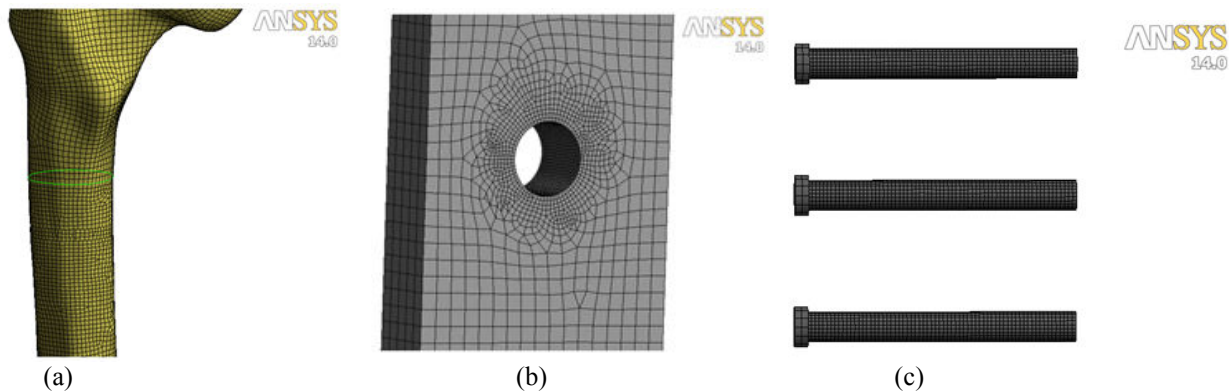


Figure 2. Mesh: (a) Bone, (b) plate (hole in detail) and (c) screws.

For frictionless contacts, the pure penalty formulation was adopted. For bounded and no separation contacts the MPC (Multi-Point Constraint) formulation was preferred because its faster solution. The bounded and the no separation contact types have the advantage to define the behavior of the faces in contact without care to the coefficient of friction. The bounded behavior is similar to a great coefficient of friction, do not allow any relative movement between the faces and the no separation type is frictionless for tangential movement, which allows slip without friction, but the faces are always in contact and cannot have separation during the analysis. The MPC is not so popular for Ansys users, like Pure Penalty and Augmented Lagrange, but it provides an efficient way to solve linear contact problems. For a more detailed description about contacts formulation applied to Ansys (Lee, 2002). The simulation was executed in two load steps: on the first step the bottom part of the bone is fixed and the bolt pretension was applied, at the second load step the static forces acting on the femur head were applied. At next section a quantitative example will be done.

3. RESULTS

The values of the forces applied on the bone, as shown in Fig. 1.a, were obtained from (Taylor, 1996). Although this reference don't explain which type of loading condition the forces are referred (standing, walking or running) it is clear that the forces values are pretty high. They are in (N): $P_A = (-1062; -130; -2800)$, $P_B = (430; 0; 1160)$, $P_C = (78; 560; 525)$ and $P_D = (0; 0; -1200)$. The distances between forces point of application and cross section centroid are (mm): $d_A = (50.7; -2.7; 218)$, $d_B = (-13.5; -6.5; 200)$, $d_C = (18.8; -29.3; 143.7)$ and $d_D = (-24.6; -4.2; 168)$. These distances and force vectors are related to the global coordinate system. The bottom side of the bone is fixed to ensure equilibrium requirements. The screw torque is set to 1 Nm and the torque coefficient is set to 0.2 (Cordey et al, 2000). The plate used in this work has $B = 4.8$ mm (thickness), $H = 16.5$ mm (width) and $L = 200$ mm (length). The bone was modeled as linear, elastic and isotropic, with $E^b = 20$ GPa, $\nu^b = 0.236$. The stain less steel plate was modeled with an elastoplastic bilinear behavior with isotropic hardening, with $E^p = 190$ GPa, $\nu^p = 0.3$, $S_y^p = 690$ MPa and $S_{ut}^p = 860$ MPa.

Note that although, from macroscopic point of view, bone can be considered non-homogeneous, porous and anisotropic, as well explained in (Doblaré et al., 2004), recent F.E. studies has shown that the constitutive simplification represented by the supposition of isotropy for long bones, instead of more realist orthotropy approach, revealed to have minor effects on principal stresses distribution at external bone surfaces (Kenedi and Vignoli, 2014). Figure 3 shows results of F.E. model application, for strain, longitudinal stress and von Mises stress.

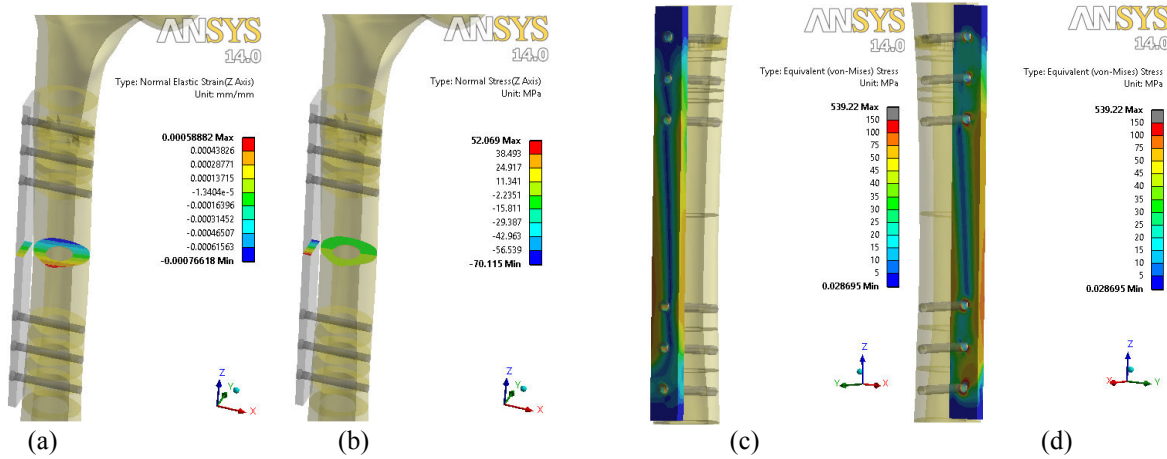


Figura 3. F.E. results: (a) longitudinal elastic strain(z axis), (b) longitudinal stress (z axis), (c) von Mises stress showing the external plate face and (d) von Mises stress showing the internal plate face (closer to cortical external bone).

Figure 3.a and 3.b, show, respectively, longitudinal elastic strain and the longitudinal stress, at a medial cross section, in both plate and bone. The plate von Mises stress distribution is presented in Fig. 3.c (external plate surface) and 3.d (internal plate surface). Note at Fig. 3.c and 3.d, at scale, there are a gray color at between 150 and 539 MPa von Mises stresses. This part of scale represents only a few punctual plate regions that hardly can be seen. The plate central region and around the holes in contact with the bone are the critical ones. Around the holes, the main problem is the contact stresses, where is also influenced by the torque applied on each bolt. On the plate central region, the stress distribution has a higher value and it can become even more critical during the healing process. Note that the von Mises stresses are higher between the internal screws and then decreases almost to zero at external screws (at plate extremities).

Figure 4 shows another way of showing F.E. results, through the utilization of paths. Figure 4.a shows a set of transversal paths that was created on the central region of the plate, assumed to be $z = 0$ mm, and four other planes that have z coordinates respectively equal to +45mm (with hole), +20mm, - 20 mm and -45mm (with hole). Another four vertical paths are shown at Fig. 4.b.

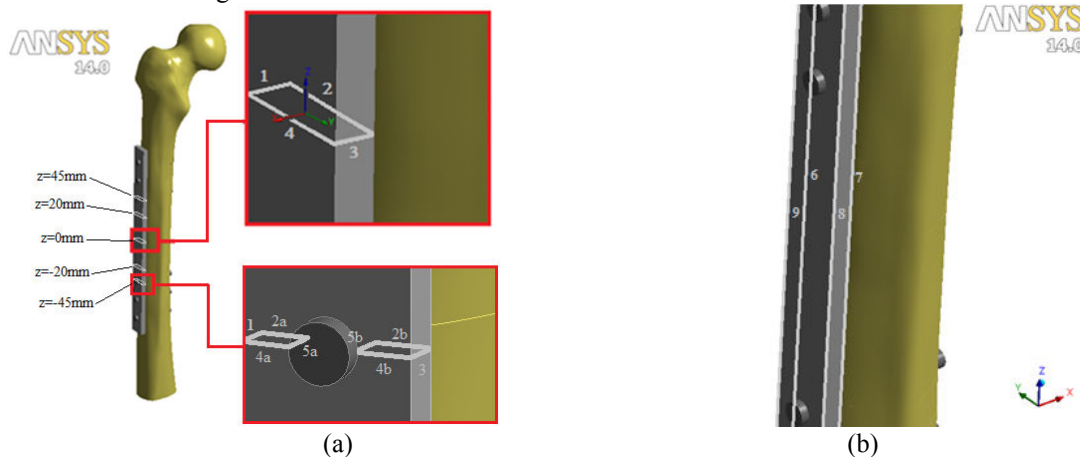


Figure 4. Paths: (a) transversal paths (for $z = 0$ mm and $z = -45$ mm are show in details) and (b) longitudinal paths.

For a more quantitative assessment, transversal paths were created at five different sections of the plate, following the numeration of Fig. 4.a. The results of the von Mises stresses along each path is plotted and compared for the five different sections at Fig. 5. Note that Fig. 5 as well as Fig.6 are plotted using the local coordinate system presented in Fig. 4 instead the global coordinate system introduced in Fig. 1. For relate this the local coordinates to the global one, one translation of $(\Delta x, \Delta y, \Delta z) = (17.83\text{mm}, 3.88\text{mm}$ and $-85.55\text{mm})$ and a rotation vector equal to $R_x = [-0.99 \ 0 \ -0.024]^T$, $R_y = [0.0011 \ -0.99 \ -0.047]^T$, $R_z = [-0.024 \ -0.047 \ 0.99]^T$ are used.

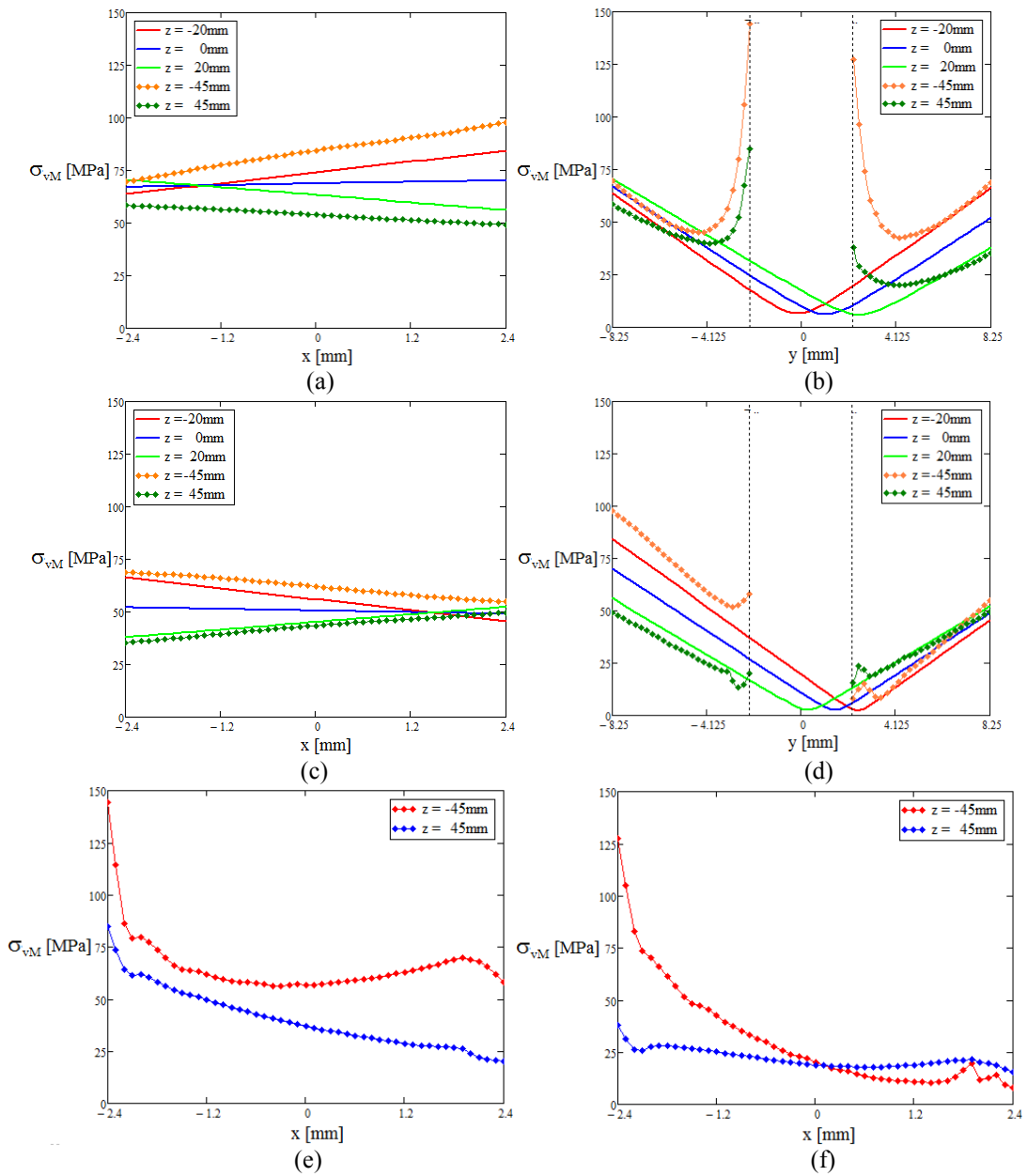


Figure 5. von Mises stress along : (a) path 1; (b) path 2; (c) path3; (d) path 4; (e) path5a and (f) path 5b.

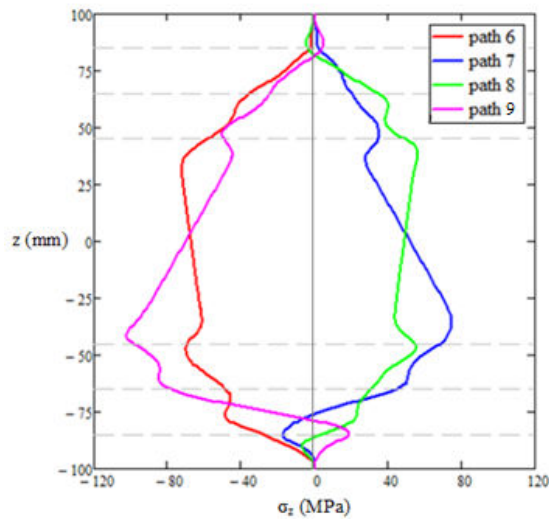


Figure 6. Normal stress along paths 6,7, 8 and 9.

According to the Fig. 5 plotted results, the bottom part of the plate has a higher stress distribution, especially at hole wall (paths 5.a and 5.b). Figure 5 shows von Mises distribution at the 5 transversal paths ($z = -45$ mm, $z = -20$ mm, $z = 0$ mm, $z = +20$ mm and $z = +45$ mm). Note that as wedges 1 and 3, Figs. 5.a and 5.c, respectively, not have significative differences between the different z . At paths 2 and 4, Figs. 5.b and 5.b, respectively have a greater von Mises Stress variation, basically as a function of bending moment influence. Note that only paths at $z = -45$ mm and $z = +45$ mm have holes, which are geometrically represented by dashed vertical lines. Also at path 5.a and 5.b, the reduced cross section area associate to stress concentration near hole walls amplifies the nominal stress approximately three times.

Figure 6 shows the longitudinal normal stress variation along the four edges of the plates with the longitudinal coordinate z . Note the screws positions are represented by dashed gray horizontal lines. This figure was plotted with normal stress instead of von Mises equivalent stress to show where the plate is in tension and where it is in compression. Note that the longitudinal stresses are higher between plate medial and distal regions, more specifically at the screw hole cross section more close to medial region, called in this work of $z = -45$ mm.

4. CONCLUSIONS

A well established F.E. software was used to study the load share between plate and bone, taking into account no femur geometry simplifications and do recognizing the plate inclination, which is necessary to adapt the plate to bone external surface. The model proposed in this paper was carried out trying to consider as much details as possible, avoiding excessive simplifications, as a result that this F. E. model can be used as reference model to be compared with analytical models, which are in development by the authors. According to the results obtained the plate presents higher stresses between medial and distal regions, more specifically at the screw hole cross section more close to medial region. One proposal to reduce this higher stresses could be an increase of cross sectional area in this region, through a gradual increase of the plate width at critical cross section.

5. REFERENCES

- Bitsakos, C., Kerner, J., Fisher, I., Amis, A.A., 2005, "The effect of muscle loading on the simulation of bone remodelling in the proximal femur", *J. of Biomechanics*, Vol. 38. p. 133-139.
- Cordey, J., Borgeaud, M., Perren, S.M., 2000, "Force transfer between the plate and the bone: relative importance of the bending stiffness of the screws and the friction between plate and bone. *Injury*", Vol. 31, Suppl. 3, p 21-28.
- Doblaré, M., García J. M. and Gómez, M. J., 2004, Modeling bone tissue fracture and healing: a review, *Engineering Fracture Mechanics*, (71), pp. 1809-1840.
- Kenedi, P.P. and Riagusoff, I.I.T., 2015, Stress development at human femur by muscle forces, *J Braz. Soc. Mech. Sci. Eng.*, Vol. 37, nº 1, pp. 31-43.
- Kenedi, P.P and Vignoli, L.L., 2014, Bone Anisotropy Influence – A Finite Element Analysis, XXIV Brazilian Congress on Biomedical Engineering – CBEB 2014, Uberlândia, Brazil.
- Lee, H. H., 2002, Finite Element Simulations with ANSYS Workbench 14, SDC Publications.
- Taylor, W.R., Roland, E., Ploeg, H., Hertig, D., Klabunde, R., Warner, M.D., Hobato, M.C., Rakotomanana, L. and Clift, S.E., 2002, Determination of orthotropic bone elastic constants using FEA and modal analysis, *J. Biomech.*, (35), pp. 767-773.
- Taylor, M.E., Tanner, K.E., Freeman, M.A.R. and Yettran, A.R., 1996, "Stress and strain distribution within the intact femur: compression or bending?", *Med. Eng. Phis.*, Vol.18, nº2, pp. 122-131.

6. RESPONSIBILITY NOTICE

The authors are the only responsible for the printed material included in this paper.